Optically detected magnetic resonance of Si donors in $Al_xGa_{1-x}As$

E. A. Montie, J. C. M. Henning, and E. C. Cosman
Philips Research Laboratories, P.O. Box 80 000, 5600 JA Eindhoven, The Netherlands
(Received 19 March 1990; revised manuscript received 19 July 1990)

Magnetic resonance signals detected both on visible and on infrared luminescence bands from Si-doped $Al_xGa_{1-x}As$ samples are described. Most samples show two superimposed resonance signals: a four-line hyperfine pattern and a single line. In this paper we focus on the single-line spectrum, which can be attributed to the Si donor system. The results, particularly the dependence of the g values and the linewidth on the aluminum content of the samples, are explained in terms of effective-mass theory. The resonance is concluded to occur in the donor level D_3, with mixed X, L, and Γ character in a local symmetry C_2 or lower. A reduced intensity of the signal in the σ^- component of the visible luminescence in heavily doped samples is explained in terms of an anomalous relaxation mechanism.

I. INTRODUCTION

The electrical conduction of n-type $Al_xGa_{1-x}As$ is commonly described in an empirical way by introducing an effective-mass shallow donor and a second deeper donor.[1] A model for this deep donor was first presented by Lang and Logan,[2] who named it "*DX* center." Obviously, a thorough understanding of the $Al_xGa_{1-x}As$ donor system is needed to explain its electrical behavior. Spectroscopic studies of Si-doped $Al_xGa_{1-x}As$ by Henning *et al.*[3-5] revealed the existence of four effective-mass donors, tied to the L, X, and Γ minima of the conduction band, in agreement with a theorem of Bassani *et al.*[6] The four donors, labeled D_1 through D_4, can be observed through their respective donor-acceptor (D-A) recombination bands in photoluminescence spectra of $Al_xGa_{1-x}As$ samples. In Fig. 1 the luminescence energies of these bands[4] are presented as a function of the aluminum content x. The figure clearly shows how the donors track the conduction band minima.

To obtain more information on the donor system, optically detected magnetic resonance (ODMR) measurements were performed by the present authors[7] and, simultaneously, by Kennedy *et al.*[8-11] Later, ODMR results were also presented by Fockele *et al.*,[12] and electron spin resonance (ESR) results were reported by Mooney *et al.*,[13] Kaufmann *et al.*,[14] and von Bardeleben *et al.*[15] Although initially the interpretation of the results varied, it is now generally agreed that one particular signal observed in both ESR and ODMR spectra is connected with Si donors. More precisely, recent measurements of the anisotropy of the signal by Glaser *et al.*[9] indicated that this resonance in fact occurs in the D_3 donor, tied to the X minimum of the conduction band. So far however, no model has yet been able to describe all features of the observed signals. In particular, the dependence of the g values and the linewidth of the resonance on the aluminum content of the sample has not been understood.

In this paper, we present the results of our ODMR study of Si-doped $Al_xGa_{1-x}As$. We also present a theoretical description of the g factor and linewidth of the magnetic resonance in an effective-mass donor with mixed X, L, and Γ character. This model successfully explains the experimental observations.

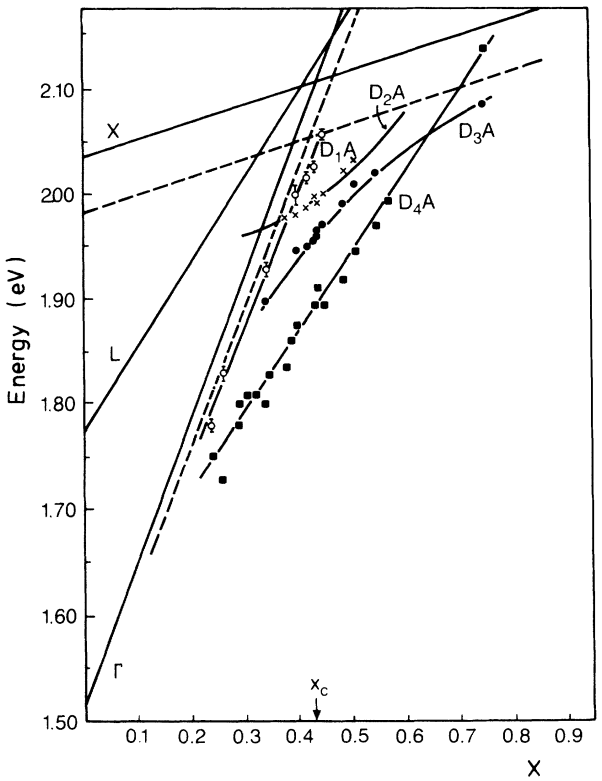

FIG. 1. Energies of the donor-acceptor luminescence bands related to the four effective-mass donors in $Al_xGa_{1-x}As$ as a function of the aluminum content. The energy positions of the conduction band minima with respect to the valence band are drawn for comparison. Dashed lines indicate the position of donor-bound excitons.

II. EXPERIMENTS

A. Experimental conditions

The samples used in our experiments were $Al_xGa_{1-x}As$ epilayers, grown either by metal-organic vapor-phase epitaxy (MOVPE) or by molecular beam epitaxy (MBE) on n^+-type or semi-insulating GaAs(001) substrates. The layers were Si-doped or not intentionally doped. Hall and capacitance-voltage (C-V) measurements at room temperature indicated donor concentrations ranging from below 1×10^{16} to 1×10^{19} cm^{-3}. The aluminum content x of the layers was determined by x-ray double-crystal diffractometry.[16]

Some samples were implanted with ^{29}Si. Several energies ranging from 50 to 700 keV were used to obtain a profile homogeneous over the entire thickness of the $Al_xGa_{1-x}As$ layer. The implanted samples were given a close-contact annealing[17] treatment for 20 minutes at 800 °C. Some properties of the samples used for this work are summarized in Table I.

Photoluminescence measurements were performed in a He bath cryostat at 1.5 K. For optical excitation an Ar^+ laser operating at 514.5 nm was used, with a typical excitation power incident on the sample of 10 W/cm^2 modulated at 300 Hz. The luminescence was detected using a photomultiplier with a cooled GaAs cathode or a cooled Ge detector, depending on the wavelength, and a 0.75-m grating monochromator.

The ODMR experiments were performed with the same equipment at 1.5 K in X-band spectrometers, in Faraday (detection along the magnetic field) or Voigt (detection perpendicular to the magnetic field) configuration. The Faraday configuration was used for all polarization studies described here. A traveling wave tube amplifier was used to attain microwave powers up to 4 W. Changes in the polarization or intensity of the luminescence induced by the microwaves, chopped at 300 Hz, were detected using a lock-in amplifier. Digital averaging was sometimes used to improve a poor signal-to-noise ratio.

B. Results

Figure 2 shows a luminescence spectrum obtained from an $Al_{0.38}Ga_{0.62}As$ sample. Just beyond 600 nm, the D_1-A and D_4-A luminescence bands are visible. The D_2-A and D_3-A bands cannot be distinguished separately in this spectrum. In addition to these bands related to the effective-mass donors, a strong emission at 1.5 μm is observed. We observe this band in most of our samples, but not in all of them. Similar luminescence bands have been reported by Kennedy *et al.*[8,9] and Fockele *et al.*[12] This 1.5-μm luminescence originates from the $Al_xGa_{1-x}As$

TABLE I. Aluminum content, net donor concentration, Hall concentration, 1.5-μm luminescence intensity, g values, and resonance linewidth of the samples used in the ODMR experiments. The g values are along the z direction unless specified otherwise. MBV- and G-numbered samples are MBE grown, all other samples are grown by MO-VPE.

Sample	x (%)	N_D-N_A (cm^{-3})	n_H (300 K) (cm^{-3})	$I_{1.5}$ (a.u.)	g	ΔB (G)
1	38	1×10^{16}		3	1.943±0.006	125±15
2	39	3×10^{17}		4	1.947±0.006	125±20
3	51	$\sim10^{16}$		1	1.955±0.003	94±6
3[a]	51	5×10^{16}		1	1.955±0.003	94±6
3[a]	51	1×10^{19}		2	1.955±0.003	94±6
4	49		5×10^{17}	3	1.954±0.004	97±5
5	55			2	1.959±0.002	83±5
6	59	$10^{17}-10^{18}$		1	1.961±0.002(z)	78±5
					1.959±0.002(y)	
					1.925±0.002(x)	
7	65	$10^{17}-10^{18}$		5	1.965±0.002	70±5
8	70	$10^{17}-10^{18}$		1	1.969±0.002(z)	65±5
					1.964±0.002(y)	
					1.921±0.002(x)	
MBV1[b]	75			1	1.971±0.002	113±20
9[c]	35			10	1.95 ±0.02	200±40
10[d]	65	-1×10^{14}		2		
10[a]	65	1×10^{19}		2	1.964±0.004	65±7
G1	40	3×10^{16}		0		
G2	40	1×10^{18}		0	1.943±0.006	110±15

[a]Si-implanted and annealed.
[b]Poor quality sample.
[c]50-μm layer detached from substrate.
[d]p type.

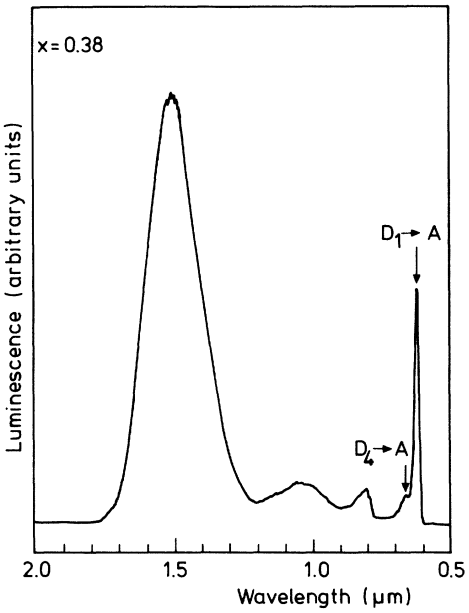

FIG. 2. Luminescence spectrum of an $Al_{0.38}Ga_{0.62}As$ sample (1), recorded at 1.5 K.

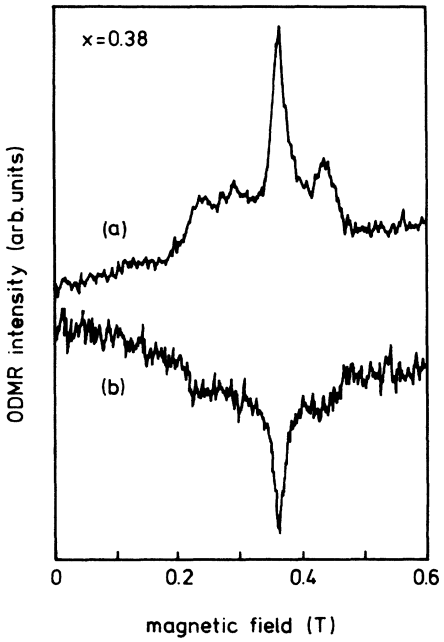

FIG. 3. ODMR spectrum of the $Al_{0.38}Ga_{0.62}As$ sample of Fig. 2 (1), detected on the 1.5-μm luminescence band (a) and on the near-band-edge luminescence (b), at 1.5 K, microwave frequency 9.681 GHz.

epilayer itself, as it disappears when excitation below the $Al_xGa_{1-x}As$ band gap but above the GaAs substrate band gap is applied. Also, the band is found in epilayers which have been removed from their substrates by chemical etching. The bands at 0.8 and 1.05 μm do originate from the substrate. The correlation between the 1.5-μm luminescence intensity and the Si doping which we have found in the first few samples investigated,[7] was apparently coincidental, and does not hold over a large number of samples (see Table I).

In Fig. 3(a) an ODMR spectrum detected on the 1.5-μm band shown in Fig. 2 is presented. The spectrum consists of a single narrow peak near 3600 G ($g \simeq 2$) superimposed on a border hyperfine split four-line spectrum. This four-line spectrum does not show shoulders due to the presence of two Ga isotopes, as in the Ga interstitial spectrum reported by Kennedy *et al.*,[8] but closely resembles the spectrum attributed to an As antisite by Fockele *et al.*[12] Our main concern in this paper will be with the sharp line. The ODMR signals detected on the infrared luminescence are positive in all our samples, i.e., the luminescence intensity increases when the microwave power is turned on. There is no difference in the signals detected on the circularly polarized components σ^+ and σ^- of the infrared luminescence separately.

The same ODMR spectrum can be detected on the near-band-edge luminescence, as is shown in Fig. 3(b), but now with the sign reversed (luminescence quenching). This is possible only with those samples which show relatively strong D_3 and D_4 related luminescence bands, which are necessary to obtain a sufficient signal-to-noise ratio. By using filters, it was established that the ODMR signals are not present in the D_1 luminescence band. At higher x values only the D_3 and D_4 bands are present, but due to the large overlap and low intensity of the bands, we could not accurately determine which of them was the source of the signals.

The ODMR signal is present in the σ^+ component of the visible luminescence, but is much weaker in the σ^- component. To investigate the influence of the concentration on this polarization effect, two pieces of an $Al_{0.51}Ga_{0.49}As$ sample (3 in Table I) were implanted with a high and a low Si dose, respectively, and subsequently annealed. The ODMR spectra detected on the σ^+ and σ^- components of the near-band-edge luminescence of these samples are shown in Fig. 4. In the lightly doped sample, the signal is observed with equal intensity in both components of the luminescence. In the heavily doped sample, however, the signal in the σ^- component is clearly weaker. Apparently, this reduction of the intensity is caused by the high donor density. The fact that the σ^+ and σ^- signals have the same sign implies a nonequilibrium distribution over the Zeeman levels of the donor-acceptor pairs.[18]

The characteristics of the ODMR signal depend on the aluminum content x of the epilayer. In Fig. 5 the dependence of the linewidth on x is presented. The line is very broad near $x \simeq 0.35$, and gets narrower with increasing x. This enables a more accurate study of the ODMR signals at higher x values. The solid line presents a fit to the theory, which will be explained in the next section

At higher x values an anisotropy of the ODMR spectrum can be observed. Figure 6 shows how the single line splits when the magnetic field is rotated from the [001] direction of growth to a [100] direction in the plane of the epilayer. Figure 7 shows the splitting of the line upon rotation of the magnetic field in the plane of the epilayer,

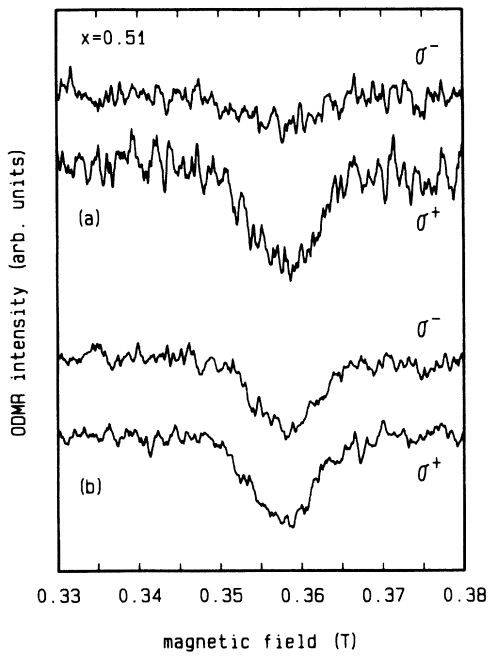

FIG. 4. ODMR spectrum of an $Al_{0.51}Ga_{0.49}As$ sample (3), detected on the two circularly polarized components σ^+ and σ^- of the near-band-edge luminescence after Si implantation to a level of 1×10^{19} (a) and 5×10^{16} (b). Temperature 1.5 K microwave frequency 9.681 GHz.

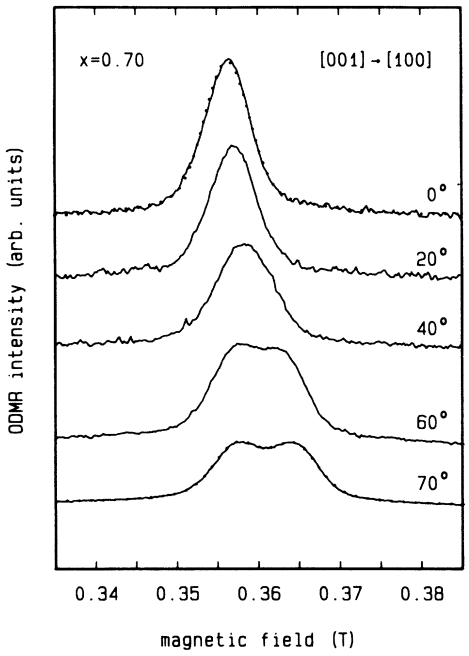

FIG. 6. Angular dependence of the ODMR spectrum of an $Al_{0.7}Ga_{0.3}As$ sample (8), recorded at 1.5 K, microwave frequency 9.681 GHz. The magnetic field is rotated from the [001] (0°) towards the [100] (90°) direction. The dotted curves are least-squares fits with Gaussians.

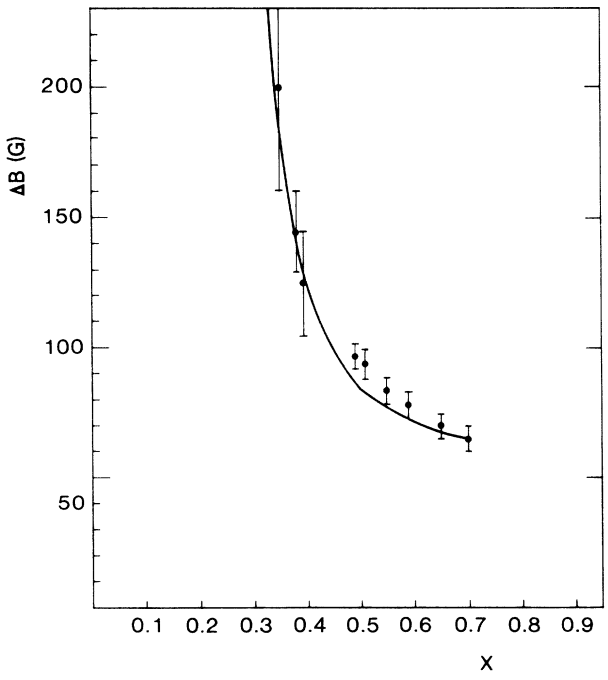

FIG. 5. Width of the ODMR line as a function of the $Al_xGa_{1-x}As$ composition. The solid line is a fit to Eq. (16).

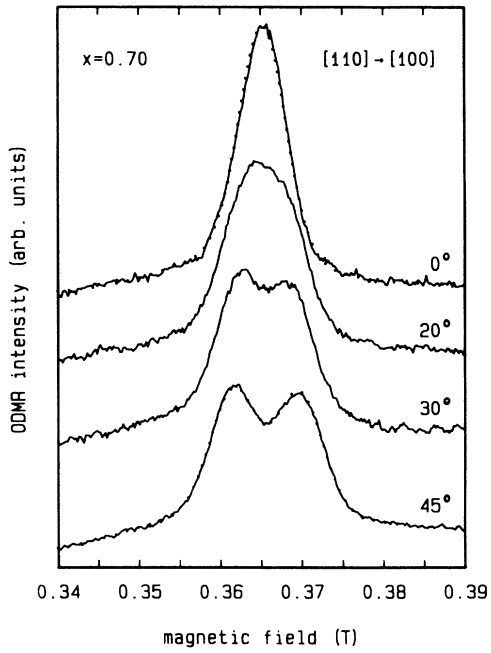

FIG. 7. Angular dependence of the ODMR spectrum of an $Al_{0.7}Ga_{0.3}As$ sample (8), recorded at 1.5 K, microwave frequency 9.938 GHz. The magnetic field is rotated from the [110] (0°) towards the [100] (45°) direction. The dotted curves are least-squares fits with Gaussians.

from a [110] to a [100] direction. In both figures, the dotted lines represent a least-squares fit to the data using Gaussians. These results clearly point to the existence of two equivalent centers, connected by the symmetry operations of the crystal class. The g tensors have predominantly axial symmetry along the [100] and [010] directions, respectively, with a small orthorhombic component at lower x values. The g value collected along the $\langle 100 \rangle$ cubic axes are listed in Table I. This anisotropy is identical with that described by Glaser *et al.*[9] Due to the increasing linewidth, it is not possible to determine the anisotropy or the main axes of the g tensor accurately for $x \lesssim 0.5$ with X-band microwaves.

The g values collected along the cubic axes g_x, g_y, g_z, (where x,y,z refer to the cubic axes [100], [010], and [001], respectively), are presented as a function of x in Fig. 8. The line can not be observed when the aluminum content is below 35%, due to the strong increase in linewidth (see Fig. 5). For higher x values the splitting of the lines increases. Some data obtained by Glaser *et al.*[9] are also presented in Fig. 8 for comparison. The agreement between these data and our own is excellent. The solid lines in Fig. 8 correspond to the theory to be presented in the next section.

To determine whether the ODMR signal is connected with the effective-mass donor system or rather with some deep center (giving rise to the 1.5-μm luminescence), we have compared two MBE-grown $Al_{0.40}Ga_{0.60}As$ layers, one nominally undoped, and one doped with Si to a level of 1×10^{18} cm^{-3}. In Fig. 9 the luminescence spectra of both samples are shown. In the undoped sample the D_1 through D_4 donor-acceptor recombination bands can be clearly distinguished. In the heavily doped sample the bands are much broadened due to the spread in donor-acceptor pair distances,[19] and the intensities of the bands related to the D_2 through D_4 donor levels have strongly increased with respect to the direct D_1-A luminescence band. The 1.5-μm band was not observed in either of these samples. Nevertheless, the sharp ODMR line could be observed in the near-band-edge luminescence of the heavily doped sample (see Fig. 10). Again, it was not pos-

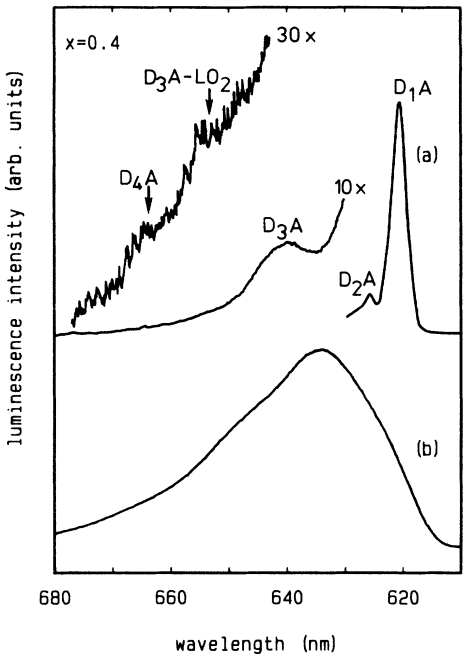

FIG. 9. Luminescence spectra of two $Al_{0.4}Ga_{0.6}As$ samples, undoped (curve *a*, sample G1) and Si doped to a level of 1×10^{18} cm^{-3} (curve *b*, sample G2). The different donor-acceptor transitions are indicated. The part of curve *a* showing the D_4A peak was obtained using selective excitation at 1.980 eV (626 nm). No 1.5-μm luminescence was observed in either of these samples.

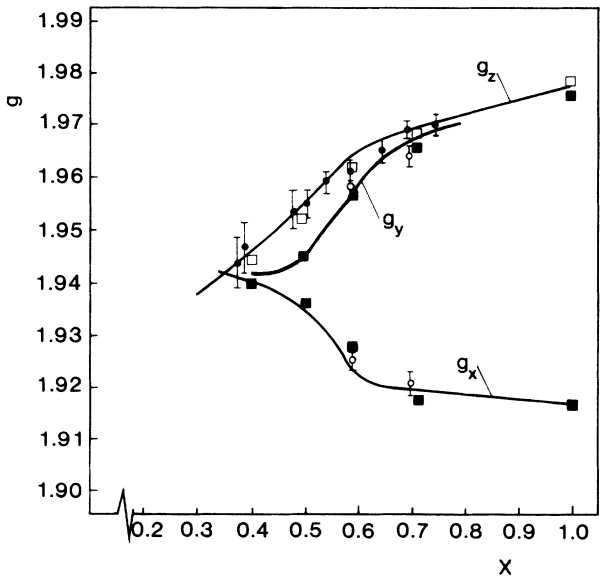

FIG. 8. Composition dependence of the observed g values. Data from Ref. 9 (□,■) have been included for comparison with our own (○,●). The g values were collected along the z axis (●,□), and along the x and y axes (○,■). The solid lines present a fit to Eq. (9).

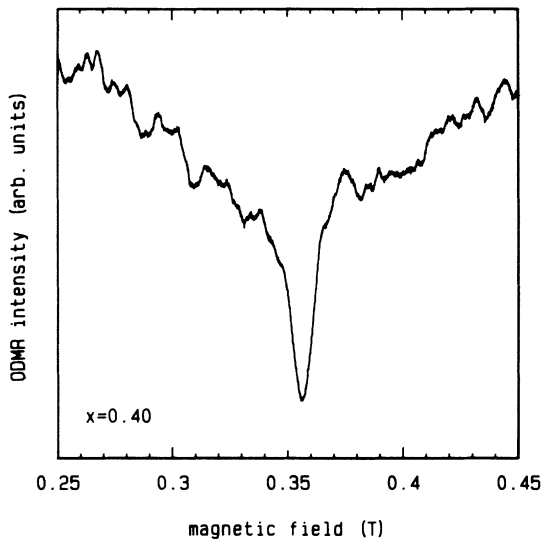

FIG. 10. ODMR spectrum detected on the near-band-edge luminescence of the heavily doped $Al_{0.40}Ga_{0.60}As$ sample of Fig. 9 (G2), recorded at 1.5 K, microwave frequency 9.681 GHz.

sible to determine from which of the bands the signal actually originates. A related experiment was done with an $Al_{0.65}Ga_{0.35}As$ sample (10 in Table I) which showed strong 1.5-μm luminescence, but no sharp ODMR line. After homogeneous implantation with ^{29}Si, to a level of 10^{19} cm^{-3}, however, the sharp ODMR line was observed clearly, while the infrared luminescence had not changed significantly.

These experiments strongly suggest that the resonance is related to one of the effective-mass donors tied to an indirect minimum of the conduction band, rather than to a deep center. The observation of the same resonance on the infrared luminescence must be due to an indirect process, in our case probably involving the As antisite.[12] A more detailed description of the supposed recombination mechanism is planned to be presented elsewhere.[20]

III. THEORY

A. Introduction

In this section we present a semiempirical theory based on effective-mass theory[21,6] (EMT) that explains the composition dependence of the g tensor and of the linewidth of the ODMR transition. The ingredients of the present theory are the following:

(1) The resonance occurs in a donor level with mixed X and L character. The X,L mixing is responsible for the composition dependence of the g values. In addition, a small Γ admixture is needed to account for the composition dependence of the linewidth $\Delta B(x)$.

(2) The X,L,Γ mixing is brought about by a low local symmetry (C_2 or lower).

(3) The single-valley g tensors have an intrinsic x dependence caused by the composition dependence of the gap, the effective masses and the spin-orbit splittings.

(4) The additional linewidth (with respect to ESR) observed in an ODMR experiment is caused by a spread in electron-hole exchange, which is proportional to the spatial extension of the wave function. The effective radius of the donor wave function is greatly influenced by a small Γ admixture.

The donor wave function is written as

$$\Psi(\mathbf{r})=a(x)\Psi^X+b(x)\Psi^L+c(x)\Psi^\Gamma \tag{1}$$

with

$$\Psi^X(\mathbf{r})=\sum_{j=1}^{6}\alpha_j\chi_j(\mathbf{r}) , \tag{2a}$$

$$\Psi^L(\mathbf{r})=\sum_{i=1}^{4}\beta_i\chi'_i(\mathbf{r}) , \tag{2b}$$

$$\Psi^\Gamma(\mathbf{r})=\chi''(\mathbf{r}) , \tag{2c}$$

$$a^2(x)+b^2(x)+c^2(x)=1 . \tag{2d}$$

The summation in Eq. (2a) is over the six equivalent X valleys: [100], [$\bar{1}$00], [010], [0$\bar{1}$0], [001], and [00$\bar{1}$]. The four L valleys occurring in Eq. (2b) are along [111], [1$\bar{1}\bar{1}$], [$\bar{1}\bar{1}$1], and [$\bar{1}$1$\bar{1}$], respectively. The $\chi_j(r)$ are the single-valley functions for the 1s donor ground state. The appropriate linear combinations $\{\alpha_j\},\{\beta_i\}$ of the valleys depend on the local point group symmetry. In what follows we restrict ourselves to donor atoms on a group III (Ga or Al) site. The minimum of the lowest conduction band at the X point then transforms according to the X_3 representation of the small point group of X.[22]

Table II shows how the single-valley donor levels are split when the local symmetry is lowered from T_d to C_2. The overall symmetry of the sample is lowered to D_{2d} by the tetragonal strain due to lattice mismatch. Further lowering of the local symmetry may be due to lattice relaxation caused by chemical rebonding, Jahn-Teller effect, random strains, alloy disorder, etc. Intervalley mixing is possible between levels that belong to the same irreducible representation of the local point group. It is readily seen that L_1-X_3 mixing can occur already in T_d symmetry. A descent in symmetry to C_2 is needed to obtain mixing between $T_2(L_1)$, $T_2(X_3)$ and $A_1(\Gamma_1)$.

B. g factor

The observed donor resonance is due to a paramagnetic center with nearly axial symmetry along one of the cubic axes $\langle 100\rangle$ lying in the epitaxial plane. For all $x>0.35$ we generally find $g_x<g_y,g_z$. For $x<0.35$ no resonance signal is observed. For $x\simeq 0.40$ the anisotropy $|g_z-g_x|$ is small. The anisotropy increases with increasing x: g_y and g_z are monotonically increasing functions of x, whereas $g(x)$ decreases monotonically with x.

In order to explain these observations we invoke the independent valley model, i.e., the spin Zeeman interaction is written as the sum of the individual contributions of each of the constituent valleys. This approach has been proven to account satisfactorily for the stress dependence of the g tensor of donors in silicon and germanium.[23,24] The g tensor is then written as

$$\begin{aligned}\mathsf{g}&=a^2\mathsf{g}^X+b^2\mathsf{g}^L+c^2\mathsf{g}^\Gamma\\&=a^2(x)\sum_{j=1}^{6}\alpha_j^2\mathsf{g}_j^X+b^2(x)\sum_{i=1}^{4}\beta_i^2\mathsf{g}_i^L+c^2(x)\mathsf{g}^\Gamma .\end{aligned} \tag{3}$$

The last term is negligible since the Γ admixture c turns

TABLE II. Splitting behavior of single-valley donor levels on descent in symmetry.

Conduction band	Point group at donor site			
minimum	T_d	D_{2d}	D_2	C_2
Γ_1	A_1	A_1	A_1	A
L_1	A_1	A_1	A_1	A
	T_2	E	B_2	B
			B_3	B
		B_2	B_1	A
X_3	T_2	E	B_2	B
			B_3	B
		B_2	B_1	A
X_1	A_1	A_1	A_1	A
	E	A_1	A_1	A
		B_1	A_1	A

out to be small and since the elements of the single-valley tensor g^{Γ} are much smaller than those of g^{L} and g^{X} as a consequence of the small effective mass at the Γ point. An *a priori* calculation of the single-valley g tensors will not be attempted here. In general their elements will depend on the aluminum content through the x dependence of the effective masses, the energy gap at the specific point in the Brillouin zone and the spin-orbit splitting.[25] For weakly x-dependent g tensors a linear expansion

$$\begin{aligned} g_{\parallel}^{X}&=g_{\parallel}^{X}(0)+k_{\parallel}^{X}x\ ,\\ g_{\perp}^{X}&=g_{\perp}^{X}(0)+k_{\perp}^{X}x\ ,\\ g_{x}^{L}&=g_{x}^{L}(0)+k_{x}^{L}x\ ,\\ g_{y}^{L}&=g_{y}^{L}(0)+k_{y}^{L}x\ ,\\ g_{z}^{L}&=g_{z}^{L}(0)+k_{z}^{L}x \end{aligned} \tag{4}$$

will be an acceptable approximation. Here $g_{\parallel}^{X}$ and $g_{\perp}^{X}$ refer to components parallel and perpendicular to the main axis of a single X valley. The experimental g data are collected along the cubic axes $\mathbf{x}=[100]$, $\mathbf{y}=[010]$ and the growth axis $\mathbf{z}=[001]$. These happen to be the principal axes of g^{X}. For arbitrary coefficients $\{\beta_i\}$ the principal axes of g^{L} will deviate from the cubic axes; hence a coordinate transformation will be necessary to obtain $g_{x,y,z}^{L}$. In what follows we will present formal expressions of the g components along the cubic crystal axes instead of along the principal tensor axes. This is done to enable a direct comparison with the experimental data of Sec. II.

It is instructive first to consider the case of local D_2 symmetry. The X_3 and L_1 wave functions transforming according to the one-dimensional representation B_1 of point group D_2 are

$$\Psi_{B_1}^{X_3}=\frac{1}{\sqrt{2}}(\chi_1-\chi_2)\ , \tag{5a}$$

$$\Psi_{B_1}^{L_1}=\tfrac{1}{2}(\chi_1'+\chi_2'-\chi_3'-\chi_4')\ , \tag{5b}$$

where the "main" twofold axis of the point group is arbitrarily chosen along [100]. Using Eq. (3) we obtain

$$\mathrm{g}=a^2(x)\begin{pmatrix} g_{\parallel}^{X} & & \\ & g_{\perp}^{X} & \\ & & g_{\perp}^{X} \end{pmatrix}+b^2(x)g_0^{L}\overleftrightarrow{I} \tag{6}$$

with

$$g_0^{L}=\tfrac{1}{3}g_{\parallel}^{L}+\tfrac{2}{3}g_{\perp}^{L}\ . \tag{7}$$

$\overleftrightarrow{I}$ is the unit dyad. For $x=1$ the X component dominates: $a(1)=1$, $b(1)=0$, and a large g anisotropy is expected as a consequence of the decoupling of the X valleys. The small anisotropy observed at moderate x values ($x\simeq 0.4$) is apparently due to the diminished influence of the X contribution. The L contribution is isotropic since the L valleys remain coupled in D_2 symmetry. The gross observations (see Fig. 8) can apparently be understood with Eq. (6). However, if we want to fit the experimental curves $g_x(x)$, $g_y(x)$ and $g_z(x)$ in detail we need more free parameters, which can be obtained by further descent in symmetry, e.g., from D_2 to C_2.

In the point group C_2 the only remaining symmetry operations are the identity and a rotation about the twofold [100] axis. The X_3 and L_1 wave functions, transforming according to the A representation read

$$\Psi_{A}^{X_3}=l_1\chi_1+l_2\chi_2+l_3(\chi_3+\chi_4)+l_4(\chi_5+\chi_6)\ , \tag{8a}$$

$$\Psi_{A}^{L_1}=p(\chi_1'+\chi_2')+q(\chi_3'+\chi_4')\ , \tag{8b}$$

In the lower point symmetry the equivalence of the four L valleys is broken and the L part of the g tensor g^{L} becomes anisotropic. This explains the small difference between g_z and g_y. Experimentally we find that this difference tends to zero for $x\rightarrow 1$ (see Fig. 8). Since the g^{X} contribution dominates for $x\simeq 1$ this implies that l_3, $l_4\simeq 0$. Equations (3), (4), and (8) lead to the following $g(x)$ values, referred to the cubic axes x,y,z:

$$g_x=a^2(x)[g_{\parallel}^{X}(0)+k_{\parallel}^{X}x]+b^2(x)[g_x^{L}(0)+k_x^{L}x]\ , \tag{9a}$$

$$g_y=a^2(x)[g_{\perp}^{X}(0)+k_{\perp}^{X}x]+b^2(x)[g_y^{L}(0)+k_y^{L}x]\ , \tag{9b}$$

$$g_z=a^2(x)[g_{\perp}^{X}(0)+k_{\perp}^{X}x]+b^2(x)[g_z^{L}(0)+k_z^{L}x]\ . \tag{9c}$$

The mixing coefficients $a(x)$ and $b(x)$ can be derived from the energy positions of the donor-to-acceptor photoluminescence transitions[4] D_2-A and D_3-A (see also Fig. 1). Their ratio can be described by the empirical formula

$$\frac{b}{a}=-0.906(1/x)^2+10.69(1/x)-15.32 \tag{10}$$

for $0.35<x<0.55$, whereas $b/a\simeq 0$ for $x>0.60$. As explained in Ref. 4, D_2 and D_3 are two donor levels with mixed L and X character. The five $g(0)$ values $g_{\parallel}^{X}(0)$, $g_{\perp}^{X}(0)$, $g_x^{L}(0)$, $g_y^{L}(0)$, $g_z^{L}(0)$ and their x derivatives $k_{\parallel}^{X}$, $k_{\perp}^{X}$, k_x^{L}, k_y^{L}, k_z^{L} are considered as adjustable parameters. They can be fitted to reproduce the experimental $g_x(x)$, $g_y(x)$ and $g_z(x)$ dependences (Fig. 8). The parameter values resulting from this fit are given in Table III. Figure 8 shows that the above sketched theory is able to explain the observed $g(x)$ dependences in a semiquantitative way, using reasonable values for the adjustable parameters. This allows us to conclude that the resonance transition observed in the ODMR experiments is due to a donor level with mixed L and X character [a slight Γ admixture is needed to explain the linewidth $\Delta B(x)$, as will be shown in Sec. III C]. The lowest donor level of this nature is the D_3 level, as observed in photoluminescence experiments.[3-5] The reason for the nonappearance of the

TABLE III. Fitting parameters used to fit Eqs. (9) and (16) to the data in Figs. 8 and 5. $H_{\Gamma L}=15$ meV, $x_c=0.27$, $\Delta B_m=62$ G.

$g_{\perp}^{X}(0)=1.950$	$k_{\perp}^{X}=+0.027$
$g_{\parallel}^{X}(0)=1.925$	$k_{\parallel}^{X}=-0.008$
$g_x^{L}(0)=1.949$	$k_x^{L}=-0.020$
$g_y^{L}(0)=1.949$	$k_y^{L}=-0.020$
$g_z^{L}(0)=1.917$	$k_z^{L}=+0.007$

deeper D_4 level in an ODMR experiment will be explained in Sec. IV.

C. Linewidth

The linewidth observed in an ODMR experiment always exceeds the ESR linewidth. This discrepancy is due to the fact that the same (e.g., donorlike) resonance transition is monitored in distinct ways in ESR and ODMR. In an ESR experiment one directly measures the rf energy loss due to the spin flip of an isolated donor. In ODMR the same donor spin flip is monitored through the change of the luminescence intensity (or polarization) of coupled donor-acceptor pairs. As a consequence of this observational technique the electron-hole exchange interaction $J_{eh}\mathbf{S}_e\cdot\mathbf{S}_h$ directly enters the resonance condition, which, e.g., for a $|M_A=\pm\frac{3}{2}, M_D=\pm\frac{1}{2}\rangle$ pair reads:

$$h\nu=g_D\mu_B B\pm\tfrac{3}{2}J_{eh} , \tag{11}$$

where $h\nu$ is the microwave energy, μ_B is the Bohr magneton, and B is the magnetic field strength. Since the donor-acceptor separation has a random distribution J_{eh} will be stochastic variable. Its contribution to the linewidth depends on the number of acceptors embraced by the donor wave function, and on the strength of the individual exchange interaction parameters. The latter do not decrease monotonically with the donor-acceptor separation, since the Bloch functions occurring in Ψ^L and Ψ^X show an oscillatory behavior. To be specific, let us consider what happens to the linewidth when x decreases from 1 to a smaller values. For $x\simeq 1$ the extension of $|\Psi(\mathbf{r})|^2$ is small, so only the first few acceptor shells can interact with the donor. The interaction is weak, however, since Eq. (8a) and 8(b) show that $|\Psi(\mathbf{r})|^2$ vanishes at the first and second neighbor positions when Ψ has mixed L and X character. When x becomes smaller, a slight admixture of Ψ^Γ is to be expected. This increases the effective radius of the donor wave function, and enhances the exchange interaction with the first and second neighbor shells. As a result the linewidth increases with decreasing x. It should be noted that this reasoning holds for small Ψ^Γ admixtures only. When the spatial extension of $|\Psi(\mathbf{r})|^2$ becomes very large, the addition of weak exchange interactions with distant acceptors will be insufficient to compensate the decrease in linewidth due to the normalization of Ψ.

A detailed quantitative description of this linebroadening mechanism is outside the scope of this paper. Instead, we will make a rather crude approximation assuming that the ODMR linewidth ΔB is proportional to the spatial extension $\langle r_D\rangle$ of the donor wave function:

$$\Delta B\propto\langle r_D\rangle=\frac{\int|\Psi(\mathbf{r})|^2 r\,d\mathbf{r}}{\int|\Psi(\mathbf{r})|^2 d\mathbf{r}} . \tag{12}$$

Inserting Eq. (1) we obtain

$$\langle r_D\rangle=\tfrac{3}{2}(a^2\langle r^X\rangle+b^2\langle r^L\rangle+c^2\langle r^\Gamma\rangle) . \tag{13}$$

Since, as a consequence of the near equality of the effective masses m_L and m_X, to a good approximation $\langle r^X\rangle\simeq\langle r^L\rangle$, this simplifies to

$$\langle r_D\rangle=\tfrac{3}{2}[(1-c^2)\langle r^L\rangle+c^2\langle r^\Gamma\rangle] . \tag{14}$$

The ratio $\rho=\langle r^L\rangle/\langle r^\Gamma\rangle$ can be estimated from the effective masses of the L and Γ valleys and amounts to $\rho=0.033$. Since $c(x)\ll 1$ we may write

$$\Delta B\propto\tfrac{3}{2}\langle r^\Gamma\rangle(c^2+0.0033) . \tag{15}$$

To first order, $c(x)$ may be approximated by $c(x)=H_{\Gamma L}/[E(D_1)-E(D_3)]$, where $H_{\Gamma L}$ is the Γ-L interaction matrix element. The unperturbed donor energies $E(D_1)$ and $E(D_3)$ are obtained from previous photoluminescence data.[4] For $0.223<x<0.70$ they can be written as $E(D_1)-E(D_3)=0.66(x-x_c)$ eV, with $x_c=0.223$. For larger x values Γ-X mixing is negligible ($c=0$). The PL data were insufficient to provide more than a rough estimate of $H_{\Gamma L}$. The definite value of this parameter and of the scaling factor ΔB_m was therefore obtained by fitting the experimental linewidth data to the expression

$$\Delta B=\Delta B_m\left[1+\frac{H_{\Gamma L}^2}{1.437\times10^{-2}(x-x_c)^2}\right] . \tag{16}$$

The fitting parameters obtained are listed in Table III. Figure 5 shows that the experimental data are reproduced well by Eq. (16). The asymptotic behavior of ΔB near $x=0.27$ is a direct consequence of the Γ admixture in the donor wave function. The enormous increase in linewidth below $x\simeq 0.3$ prohibits the observation of ODMR at low x values.

In conclusion, the composition dependence of the g factors and of the linewidth can be understood if we assume that the resonance observed in the ODMR experiment takes place between Zeeman sublevels of the D_3 donor level with mixed X, L, and Γ character. The local site symmetry is not higher than C_2.

IV. DISCUSSION

Our ODMR results are in good agreement with ODMR as well as ESR results obtained by other groups.[8–15] The sign of the ODMR signals detected on the infrared luminescence bands is positive in all of our samples. Kennedy *et al.*[8] have observed both positive and negative signals in different luminescence bands from the same sample. Clearly, the sign of the signals depends on the particular indirect process through which the resonance is observed. The resonance itself, however, is the same in all cases, and is apparently not influenced by these processes. Our results concerning the presence of the ODMR signal in the near-band-edge luminescence of $Al_xGa_{1-x}As$ samples suggest that the resonance in fact occurs in the effective-mass donor system, in the D_3 or D_4 to be more precise.

Unfortunately, we were unable to decide on experimental grounds whether D_3 or D_4 is the ODMR-active donor

level. The reason is that the doping level of the samples suitable for ODMR is rather high, so that the PL transitions D_3-A and D_4-A overlap strongly. The theory presented in Sec. III, however, suggests D_3 is the active level. This is in full agreement with the conclusions of Refs. 9, 10, 13, and 14.

The nonobservation of ODMR in the lowest state D_4 is less paradoxical than it might appear at first sight. One should realize that ODMR is essentially a nonequilibrium experiment in which the donor levels are partially emptied by strong illumination. The residual occupation of the donor levels in this dynamic equilibrium is governed by the balance between electron capture and photoionization. Earlier luminescence[4] and photoconduction[5] experiments have shown that at low temperatures the capture rate of D_4 is much smaller than that of the levels D_1, D_2 and D_3. An estimate[5] of the capture cross section $\sigma_c(D_4)=4\times10^{-24}$ cm^2, valid below 100 K, shows that a very weak occupation of the D_4 level can indeed be expected even on moderate illumination.

The linewidths obtained in ESR measurements[13–15] are smaller than those obtained in ODMR experiments. As mentioned in Sec. III, this is due to donor-acceptor exchange interaction. The linewidths obtained by Kennedy *et al.*[8–11] are about 20 G above our linewidths. We attribute this difference to the higher microwave frequency used in their experiments (24 versus 10 GHz). This frequency-dependent component of the linewidth, due to a spread in g values, is negligible in our results, and donor-acceptor exchange may safely be considered as the main broadening mechanism. Indeed the expression derived for the linewidth depending on the composition [Eq. (16)] based on a spread in donor-acceptor exchange describes our results accurately (see Fig. 5).

The g values obtained from ODMR and ESR experiments are in excellent agreement, in spite of the differences in the sample properties and observation mechanism. This proves that the donor system in which the resonance occurs is a well defined physical system, suitable for modeling.

The anisotropy of the ODMR spectra we observed is the same as that described by Glaser *et al.*[9] As they pointed out, it is compatible with the behavior expected from electrons in the X_X and X_Y valleys of the conduction band, which are lowered with respect to the X_Z minimum due to the biaxial misfit strain. The same situation was found in type-II GaAs/AlAs quantum wells.[26] The fact that the X_X and X_Y valleys are observed separately with equal intensity means that the local symmetry must be lowered even further, e.g., by one of the mechanisms mentioned in Sec. III A. This was also pointed out by Kaufmann.[14] An effective-mass donor tied to the X minimum of the conduction band, in a low local symmetry and with additional X-L-Γ mixing is exactly the model system described in Sec. III. The agreement between the linewidths and—more importantly—the g values obtained from the model and from experiments is excellent. This leads us to the conclusion that this description is correct.

An alternative theory has been presented by Glaser *et al.*[11] In this theory it is supposed that the physical basis of the apparent x dependence of g is in fact a dependence on the misfit strain in the epilayers, which indeed increases with increasing x. The main drawback of this theory is that it predicts a $1/x^2$ dependence for g_z, and a mixed $1/x$, $1/x^2$ dependence for g_x and g_y. Figure 8 shows that this is in contradiction with the abundant experimental data now available. Moreover, this theory is unable to explain the x dependence of the linewidth. Finally it should be remarked that one of the data points in Figs. 5 and 8 refers to a 50-μm-thick $Al_{0.35}Ga_{0.65}As$ layer, which was detached from its GaAs substrate. Although the misfit strain in this sample will be strongly reduced with respect to "normal" samples, neither the g value nor the linewidth deviates from the behavior predicted by Eq. (9) and (16). This throws doubt on the predominant influence of misfit strain on $g(x)$ and $\Delta B(x)$ supposed in Ref. (11).

The reduced intensity of the ODMR signal in the σ^- component of the visible luminescence in heavily doped samples is intriguing. A possible explanation in terms of anomalous relaxation effects has been proposed in an earlier publication.[7] An extension of the work by Fraenkel and co-workers,[27,28] originally devised for free radicals in solution, shows that two characteristics of the donor resonance, namely the spin-lattice relaxation time T_1 and the linewidth parameter T_2 depend on the magnetic quantum number M_A of the acceptor:

$$\frac{1}{T_{1,2}}=KM_A^2+LM_A+N\ , \tag{17}$$

provided that suitable time-dependent interactions are present that induce transitions between spin levels. Such interactions can exist in an n-type semiconductor when the donor wave functions overlap strongly enough to form a donor band. The hopping of the donor electron then leads to correlated fluctuations of the anisotropic parts of the donor g tensor and the electron-hole exchange $\mathbf{J}_{eh}$, a prerequisite for the occurrence of a nonvanishing coefficient L. If, in addition, the hopping correlation time τ_c is smaller than the luminescence lifetime τ_f one of the two possible donor resonances[7] (e.g., $M=-2\rightarrow M=-1$) is preferentially broadened or weakened and the resonance signal in the σ^- component of the recombination radiation may disappear.

The results in Fig. 4 support this explanation. In accord with the expectations we find that the ODMR signal is much weaker in the σ^- component of the luminescence of the heavily doped sample, whereas it shows up in both the σ^- and σ^+ polarizations in the lightly doped sample. The latter sample has a doping level low enough to avoid D_3-donor band formation. It is interesting to note that very lightly doped samples also do not show persistent photoconductivity.[5] This suggests that the occurrence of persistent photoconductivity requires the existence of a donor impurity band, in agreement with a suggestion made by Hjalmarson and Drummond.[29]

In summary, we have performed ODMR measurements with Si-doped $Al_xGa_{1-x}As$ samples. The single-

line spectrum, detected on both near-band-edge and deep luminescence bands, is attributed to a resonance in the Si donor system. The anisotropy of the spectra, and the composition dependence of the g values and the linewidth can be explained by a model based on effective-mass theory. The resonance is concluded to occur in the donor level D_3, with mixed X, L, and Γ character in a local symmetry C_2 or lower. Anomalous relaxation effects due to donor band formation are observed at high donor concentrations.

ACKNOWLEDGMENTS

We are grateful to P. J. Roksnoer, C. T. Foxon, J. J. Harris, J. W. F. Maes, and K. Heime for providing samples, to E. H. A. Dekempeneer and J. Politiek for the implantation of some samples, and to M. B. M. Kemp for subsequent annealing. Valuable discussions and the exchange of results prior to publication with Q. H. F. Vrehen, R. P. van Stapele, E. Glaser, T. A. Kennedy, M. Fockele, J. M. Spaeth, F. Hofman, and U. Kaufmann are gratefully acknowledged.

[1]A. J. Springthorpe, F. D. King, and A. Becke, J. Electron. Mater. **4**, 101 (1975).
[2]D. V. Lang and R. A. Logan, Phys. Rev. Lett. **39**, 635 (1977).
[3]J. C. M. Henning and J. P. M. Ansems, Semicond. Sci. Technol. **2**, 1 (1987).
[4]J. C. M. Henning, J. P. M. Ansems, and P. J. Roksnoer, Semicond. Sci. Technol. **3**, 361 (1988).
[5]J. C. M. Henning, in *DX Centers in GaAs Alloys,* edited by J. C. Bourgoin (Sci-Tech, Vaduz, 1990), p. 145.
[6]F. Bassani, G. Iadonisi, and B. Preziosi, Phys. Rev. **186**, 735 (1969); Rep. Prog. Phys. **37**, 1099 (1974).
[7]E. A. Montie and J. C. M. Henning, J. Phys. C **21**, L311 (1988).
[8]T. A. Kennedy, R. Magno, and M. G. Spencer, Phys. Rev. B **37**, 6325 (1988).
[9]E. Glaser, T. A. Kennedy, R. S. Sillmon, and M. G. Spencer, Phys. Rev. B **40**, 3447 (1989).
[10]T. A. Kennedy and E. Glaser, in *DX Centers in GaAs Alloys,* edited by J. C. Bourgoin (Sci-Tech, Vaduz, 1990), p. 53.
[11]E. Glaser, T. A. Kennedy, and B. Molnar, Inst. Phys. Conf. Ser. **95**, 233 (1989).
[12]M. Fockele, B. K. Meyer, J. M. Spaeth, M. Heuken, and K. Heime, Phys. Rev. B **40**, 2001 (1989).
[13]P. M. Mooney, W. Wilkening, U. Kaufmann, and T. F. Kuech, Phys. Rev. B **39**, 5554 (1989).
[14]U. Kaufmann, W. Wilkening, P. M. Mooney, and T. F. Kuech (unpublished).
[15]H. J. von Bardeleben, J. C. Bourgoin, P. Basmaji, and P. Gibart, Phys. Rev. B **40**, 5892 (1989).
[16]W. Bartels and H. Veenvliet, in *Proceedings of the Conference on Gallium Arsenide and Related Compounds, St. Louis, 1978,* edited by C. M. Wolfe [Inst. Phys. Conf. Ser. **45**, 229 (1979)].
[17]B. Molnar, Appl. Phys. Lett. **36**, 927 (1980).
[18]J. J. Davies, J. Phys. C **16**, L867 (1983).
[19]W. Hoogenstraten, Philips Res. Rep. **13**, 515 (1958).
[20]M. Fockele, J. M. Spaeth, E. A. Montie, and J. C. M. Henning (unpublished).
[21]J. M. Luttinger and W. Kohn, Phys. Rev. **97**, 869 (1955).
[22]T. N. Morgan, Phys. Rev. Lett. **21**, 819 (1968).
[23]D. K. Wilson and G. Feher, Phys. Rev. **124**, 1068 (1961).
[24]D. K. Wilson, Phys. Rev. **134**, A265 (1964).
[25]L. Roth, Phys. Rev. **118**, 1534 (1960).
[26]H. W. van Kesteren, E. C. Cosman, P. Dawson, K. J. Moore, and C. T. Foxon, Phys. Rev. B **39**, 13 426 (1989).
[27]J. W. H. Schreurs and G. K. Fraenkel, J. Chem. Phys. **34**, 756 (1961).
[28]M. J. Stephen and G. K. Fraenkel, J. Chem. Phys. **32**, 1435 (1960).
[29]H. P. Hjalmarson and T. Drummond, Appl. Phys. Lett. **48**, 646 (1986).